

# DESIGN OF A COMPACT LINAC FOR HIGH AVERAGE POWER RADIOTHERAPY\*

C. D. Nantista<sup>†,1</sup>, G.B. Bowden<sup>1</sup>, Z. Li<sup>1</sup>, M. Shumail<sup>1</sup>, S.G. Tantawi<sup>1</sup> and B.W. Loo<sup>2,3</sup>

<sup>1</sup>SLAC National Accelerator Laboratory, Menlo Park, USA

<sup>2</sup>Department of Radiation Oncology, Stanford University School of Medicine, USA

<sup>3</sup>Stanford Cancer Institute, Stanford University School of Medicine, USA

## Abstract

We present the design of a compact, 10 MeV, 300 mA pulsed X-band linac developed for medical application. The layout, <1 m including gun, buncher, capture section and current monitor, is of a recent configuration in which the 36 main linac cavities are individually fed in parallel through side waveguide manifolds, allowing for split fabrication. Initially destined for experimental study of FLASH irradiation of mouse tumors, the design was developed as a prototype for realization of a PHASER cancer treatment machine, in which multiple linacs, powered sequentially from a common RF source, are to provide rapid treatment to patients from multiple directions without mechanical movement, delivering dosage on a time scale that essentially freezes the patient. In this paper, we focus on the RF design, beam capture optimization, mechanical design and fabrication of the linac itself, deferring discussion of other important aspects such as window and target design, experimental specification setting, radiation shielding and operations.

## INTRODUCTION

A fundamental goal for improving the effectiveness of radiation therapy for curing cancer is maximizing the differential damage done to cancerous tumors and normal tissue. To this end, so-called FLASH radiotherapy, with greatly enhanced dose rates (>50 Gy/s), promises significant advantages, used in conjunction with modern imaging and localization techniques. Rapid dose delivery effectively addresses the problem of “motion management”.

A revolutionary platform for implementing multidirectional FLASH treatment has been proposed [1]. Dubbed PHASER (Pluridirectional High-energy Agile Scanning Electronic Radiotherapy), it employs multiple (16) electron linacs, arrayed to target a common point and fired in sequence, thus eliminating the need for gantry motion.

The linacs for this scheme are required to compactly produce pulsed 300 mA, 10 MeV electron beams. We briefly describe here the effort toward developing such a linac at X-band using a distributed coupling approach [2], in which the cavities are individually powered from side manifolds.

## LINAC ANATOMY

The overall RF layout of the PHASER linac vacuum space between the 30 kV electron gun and the target (neither shown) is illustrated in Fig. 1. It consists of a buncher cavity, a 5-cell single-feed capture section and a 36-cavity distributed-coupling main linac with two side manifolds,

followed by a current monitor cavity. On either side of the capture section is a drift space where the beam tube is surrounded by a solenoidal permanent magnet for focusing. The operating frequency is 11.424 GHz, and the beam is bunched and accelerated from a 30 kV gun up to 10 MeV in 26 inches (0.66 m), an effective gradient of ~15 MV/m.

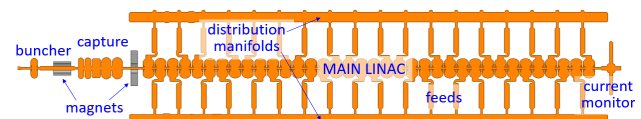


Figure 1: Linac RF design vacuum space.

## CAVITY DESIGN

### Main Linac Cavities

By eliminating the need for cell-to-cell coupling through the beam iris, the distributed coupling paradigm, like off-axis coupling schemes, allows greater freedom in cavity shape design, in particular allowing nose cones and a small beam aperture. For the main linac, cavity shapes were designed using an organic optimization code that maximizes shunt impedance while limiting peak surface fields related to RF breakdown, thus providing both good acceleration efficiency and high-gradient capability.

While ideally cavity spacing would track beam velocity, an acceptable solution was found to utilizing only two cell types, simplifying the RF design of the linac without losing much efficiency. The cavity shapes, optimized around different beam betas, are illustrated in Fig. 2. With a beampipe radius of 1 mm, effective shunt impedances of ~200 MΩ/m are achieved. Of the 36 cavities, the first 6 are of type A and rest of type B. To further maintain the beam phasing through the π-mode structure, the spacing after each A cavity was allowed to gradually increase from 1.249 cm to a constant 1.307 cm for the B cavities.

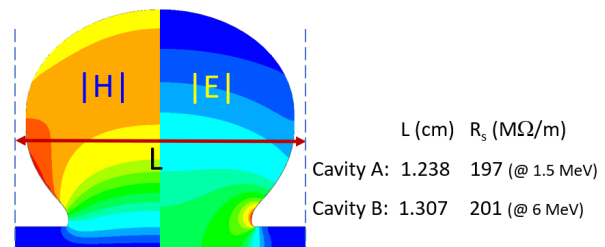


Figure 2: Main linac cavity profiles (dimensions in cm).

### Capture Section/Injector

The capture section has five iris-coupled cells, with input coupler in the center cell. The outer walls are fully rounded, except for the coupler cell. The cell lengths increase with

\*Work supported by a grant from Stanford University School of Medicine.  
<sup>†</sup>nantista@slac.stanford.edu

beam energy, with only the last two left identical. The geometry and the deliberately non-uniform electric field amplitude on axis are illustrated in Fig. 3. This short section helps to bunch and capture the beam current, while raising the energy of electrons destined to survive to  $\sim 0.9$  MeV.

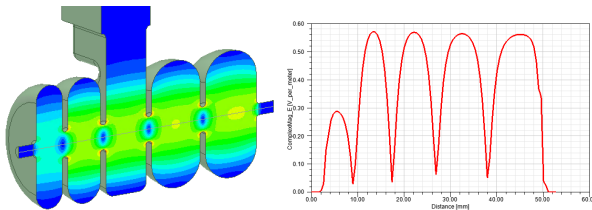


Figure 3: Capture section and field profile.

### Buncher and Current Monitor

The short buncher cavity design is illustrated in Fig. 4a. Machine tooling considerations limited its shape optimization, but with an effective shunt impedance of  $0.6 \text{ M}\Omega$ , it requires relatively little drive power ( $\sim 100 \text{ W}$ ) in our design, to be siphoned off from the linac waveguide with a 35 dB directional coupler, followed by attenuation and phase adjustment in coax.

Figure 4b shows a diagnostic cavity appended at the end of the linac to monitor the captured beam current. The goal here was to minimize shunt impedance to limit the attenuation required on the output. The beampipe radius is increased to 2 mm before opening in a radiused double step into the flat cavity. To further limit R/Q, the cavity is extended to the sides to be resonant in a  $\text{TE}_{310}$  rectangular-like mode. With a shunt impedance of  $0.15 \text{ M}\Omega$  and  $\beta$  of  $\sim 3$ , it should extract  $\sim 2.6 \text{ kW}$  peak from the 300 mA beam.

Each of these lower power cavities are coupled with a narrow waveguide tapered to a WR750 port with an incorporated ceramic vacuum window and instrument flange.

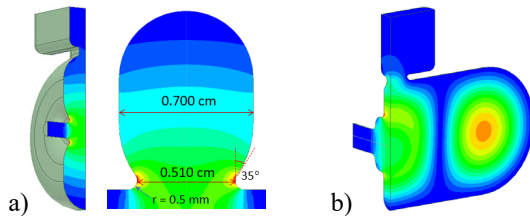


Figure 4: a) Buncher cavity and b) current monitor cavity.

## BEAM SIMULATION AND RF DESIGN OPTIMIZATION

Extensive calculations, including ASTRA beam simulations, were performed to optimize overall beam capture and to set match conditions. The spacings, RF power levels and relative phases of the sections were determined (see Table 1), as well as the magnet parameters. Within the main linac, cavity coupling betas were iteratively calculated to accommodate equal RF drive power with evolving beamloading. Power into the walls from both RF and beam loss were determined for heating considerations.

Table 1 summarizes the RF design parameters, and Fig. 5 shows field profiles along the whole linac. Figure 6a illustrates simulated current transmission through the main

linac of 79% (60% overall from the gun) and Fig. 6b shows the final energy-RF phase distribution of the captured bunches.  $\sim 89\%$  of particles are within 1% energy spread and  $\sim 95\%$  within 4% energy spread.

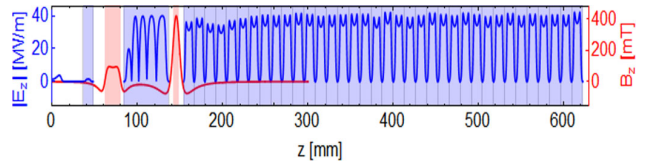


Figure 5: RF electric field and focusing magnetic field profiles along the axis of the overall linac structure.

Table 1: RF Design Parameters

Section	Power (kW)	Coupling $\beta$	Phase ( $^\circ$ )
Buncher	$0.105 \pm 0.01$	$2.74 \pm 0.12$	$166 \pm 2$
Capture	$588 \pm 5$	$2.39 \pm 0.02$	$-107.1 \pm 0.3$
C1-C6	$103.5 \pm 0.5$	3.97	$-15.7 \pm 0.4$
C7-C36	(3,726 total)	3.86	(+180 even)

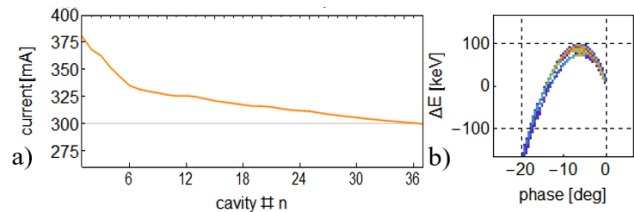


Figure 6: a) Beam current along the main linac and b) phase space of output beam bunches.

## DISTRIBUTION MANIFOLD DESIGN

The 36 main linac cavities are powered through two side waveguide manifolds. With H-plane T-junction inputs at their centers, each half manifold feeds 9 cavities. A 3-port design satisfying the scattering matrix required for constructing a 9-feed matched, equal distribution,  $180^\circ$  phase advance circuit at a feed spacing of twice the cavity B length is shown in Fig. 7a. Figure 7b shows the downstream and one upstream arm of the manifolds from the matched midpoint input junction. The slight step pairs between the left few feeds of the upstream arm are introduced to maintain matched phase length between feeds whose physical spacing is changing to follow the cavity spacing. The two upstream arms are thus not identical.

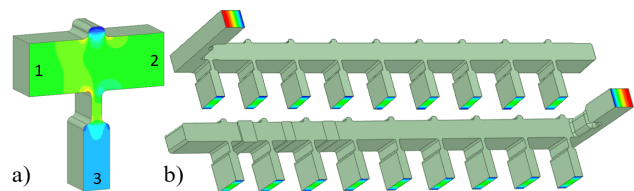


Figure 7: a) 9-feed 3-port junction design and b) downstream (top) and upstream (bottom) manifold arms.

## LOW-FIELD CAVITY COUPLING

Distributed coupling employs parallel RF power feeds into each individual cavity via a coupling hole at the high

magnetic field region. The coupling hole pushes the surface current toward the edge of the opening, which can result in significant magnetic field enhancement. The optimization approach incorporated features that enhanced coupling between the cavity and the feeding waveguide, thus reducing the opening size. Additionally, larger elliptical rounding and smaller circular rounding were used to further minimize the surface field enhancement.

With optimized coupling geometry, the field enhancement was reduced from >200% of an original design to <20%, depending on the cavity type and coupling  $\beta$ , as showing in Fig. 8. The cavity A design on the left has a coupling  $\beta$  of 3.97 and B-field enhancement of 19%, while the cavity B on the right side has a  $\beta$  of 3.85 and field enhancement of 6%, compared to the peak surface magnetic field without coupling.

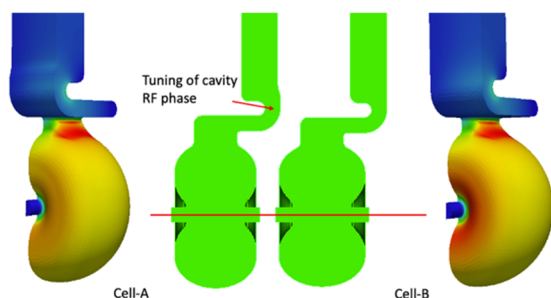


Figure 8: L-shaped coupler with minimized B surface field enhancement.

To compensate for dimensional differences and establish equal phase lengths to the cavity centers, a slight trombone feature was included in the cavity A feed, as indicated. Feed length from the manifold (or manifold spacing) is set such that when a cavity is shorted with a wire during the cavity tuning process, there is no reflection along the manifold from its feed (i.e.  $|S_{21}| = 1$  in Fig. 7a).

### INPUT RF SPLIT

The initial plan for splitting power between capture section and main linac is illustrated in the “tripod” circuit of Fig. 9a. The main junction is a magic-Tee. The bends to the manifolds are deliberately mismatched to reflect the fraction needed for the capture section, asymmetric and oppositely oriented so that the reflections incur a  $180^\circ$  phase difference and combine into the fourth port. The run to the capture feed has a tapered width section whose length is adjusted to yield the needed relative phase.

For our prototype, power will be split through a 2-hybrid / 2-phase shifter waveguide circuit, illustrated in Fig. 9b, to allow for adjustment of relative amplitude and phase. A brazed-in T then divides the main linac power between the manifolds. The height of this T (or Y) is set to avoid a choke forming between one arm and the other due to any asymmetry during filling or during cavity tuning.

### LINAC FABRICATION

The full linac structure, including distribution manifolds and gun anode, is CNC machined in halves into two  $64.8 \text{ cm} \times 14.58 \text{ cm} \times 2.03 \text{ cm}$  OFHC copper plates. Pock-

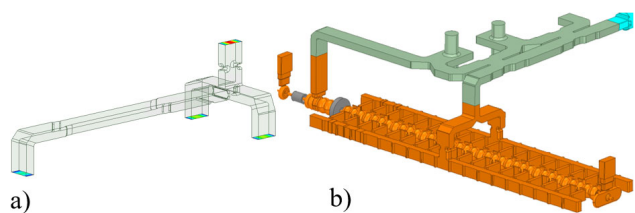


Figure 9: a) Fixed and b) variable power splitting circuits.

ets are cut through the plates at the two focusing solenoid locations. Split rare earth permanent magnets are later clamped around beampipe spools brazed across these pockets.

The plates are diffusion bonded in a hydrogen atmosphere furnace at a bond plane pressure of approximately 27 bar for 30 minutes at  $650^\circ\text{C}$ . A bolted press made of stainless plates is used to press the stacked plates together (Fig. 10a). Included in the press assembly stack is a diaphragm made of 1 mm-thick stainless-steel sheets welded together around the edges. Connected through 3 mm OD stainless steel tubing to an external 14 bar argon gas source, it is used to supply the bond pressure. All steel press surfaces are coated with a boron nitride loaded furnace release paint to prevent their bonding.

After diffusion bonding, cavity tuning pins, flanged waveguide ports, accelerator vacuum flanges and external water-cooling tubes are brazed on using Au/Cu braze alloy. A cross-section of the full accelerator with attached triode electron gun is shown in Fig. 10b.

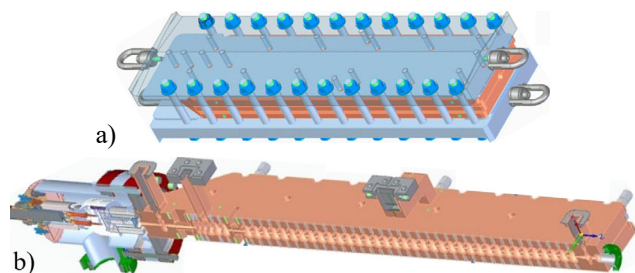


Figure 10: a) Plate diffusion bonding assembly and b) split view of linac with gun attached.

### CONCLUSION

A compact 10 MeV, 300 mA X-band linac of novel configuration and fabrication, with a 0.5% duty factor has been designed for radiotherapy application. Extensive use was made in the design process of Ansys HFSS, ACE3P, ASTRA and custom codes. It is currently in fabrication and destined for FLASH research, with an ultimate goal of incorporation in a PHASER scheme.

### REFERENCES

- [1] P.G. Maxim *et al.*, “PHASER: A platform for clinical translation of FLASH cancer radiotherapy.” *Radiotherapy and Oncology: Journal of the European Society for Therapeutic Radiology and Oncology*, vol. 139, pp. 28-33, 2019. doi:10.1016/j.radonc.2019.05.005
- [2] S. Tantawi, *et al.*, “Distributed Coupling Accelerator Structures: A New Paradigm for High Gradient Linacs”, 2018. doi:10.48550/arXiv.1811.09925